International Journal of Nanomedicine

Dovepress
open access to scientific and medical research

Open Access Full Text Article

ORIGINAL RESEARCH

Nanostructured Coating of Non-Crystalline Tantalum Pentoxide on Polyetheretherketone Enhances RBMS Cells/HGE Cells Adhesion

This article was published in the following Dove Press journal:
International Journal of Nanomedicine

Zhiying Pang[1,*]
Zhangyi Pan[1,*]
Min Ma[1]
Zhiyan Xu[2]
Shiqi Mei[2]
Zengxin Jiang[3]
Feng Yin[1]

[1]Department of Joint Surgery, Shanghai East Hospital, School of Medicine, Tongji University, Shanghai 200092, People's Republic of China; [2]Key Laboratory for Ultrafine Materials of Ministry of Education, East China University of Science and Technology, Shanghai 200237, People's Republic of China; [3]Department of Orthopedic Surgery, Zhongshan Hospital, Fudan University, Shanghai 200032, People's Republic of China

*These authors contributed equally to this work

Purpose: As a dental material, polyetheretherketone (PEEK) is bioinert that does not induce cellular response and bone/gingival tissues regeneration. This study was to develop bioactive coating on PEEK and investigate the effects of coating on cellular response.

Materials and Methods: Tantalum pentoxide (TP) coating was fabricated on PEEK surface by vacuum evaporation and responses of rat bone marrow mesenchymal stem (RBMS) cells/human gingival epithelial (HGE) were studied.

Results: A dense coating (around 400 nm in thickness) of TP was closely combined with PEEK (PKTP). Moreover, the coating was non-crystalline TP, which contained many small humps (around 10 nm in size), exhibiting a nanostructured surface. In addition, the roughness, hydrophilicity, surface energy, and protein adsorption of PKTP were remarkably higher than that of PEEK. Furthermore, the responses (adhesion, proliferation, and osteogenic gene expression) of RBMS cells, and responses (adhesion and proliferation) of HGE cells to PKTP were remarkably improved in comparison with PEEK. It could be suggested that the nanostructured coating of TP on PEEK played crucial roles in inducing the responses of RBMS/HGE cells.

Conclusion: PKTP with elevated surface performances and outstanding cytocompatibility might have enormous potential for dental implant application.

Keywords: polyetheretherketone, tantalum pentoxide, nanostructured coating, cytocompatibility, dental implant applications

Introduction

Dental implants are surgically placed into the upper or lower jaw, where they function as a fixture for replacing missing teeth.[1] The success of dental implants requires integration with not only bone tissue to achieve osteointegration but also gingival tissues to obtain biological sealing that maintains the long-term stability of implants.[1,2] Dental implants are commonly made of titanium (Ti) and its alloys.[3] However, due to the high modulus of elasticity, Ti-based implants generate stress-shielding, which leads to periodontal bone resorption, and thereby causing loosening, and even failure of implants.[3,4] In addition, because of corrosion, the slow release of some metal ions (eg, aluminum and vanadium) from Ti-based implants may be toxic to the human body.[5] Polyetheretherketone (PEEK) with outstanding mechanical strengths, biocompatibility, and bio-stability as well as easy processing is extensively applied as implants in dental and orthopedics.[6] The molecular backbone of PEEK includes the combination of ketone and ether groups in the aryl

Correspondence: Zengxin Jiang
Tel +86 21-64041990
Email Dr_Jiangzx@163.com

Feng Yin
Tel +86 21-64041990
Email 001yinfeng@sina.com

submit your manuscript | www.dovepress.com
DovePress
http://doi.org/10.2147/IJN.S286643

rings.[7] This peculiar structure of PEEK causes its high mechanical strength, and biostability in biological environments, which elicits no toxic, inflammatory, or mutagenic responses in the human body.[7]

Generally, Ti-based implants with high elastic modulus produce stress shielding effects that cause bone resorption, while the modulus of elasticity of PEEK approximates that of human cortical bone, thereby PEEK is a preferred implantable material to replace metal implants for dental application.[9] However, PEEK is a biologically inert material that cannot induce cell attachment, proliferation, and differentiation, as well as bone regeneration.[10] Moreover, PEEK may hardly induce osteogenesis and osseointegration.[11] Consequently, one of the challenges is to enhance the osteogenesis and osseointegration of PEEK for dental application. The surface characteristics such as composition and topography can effectively regulate the biological properties of implants.[12] Recently, PEEK has been functionalized to create a nanotopography surface, which improved surface bioactivity and other performances.[13,14] Some ways, such as plasma immersion ion implantation, electron beam deposition, gas plasma etching, and spin-coating, have been used to treat the PEEK surface at micro-nano levels to enhance its osteogenic bioactivity.[13–16] However, surface treatment of PEEK produced by these ways did not obviously improve the surface bioactivity of PEEK, which exhibited low osteogenic bioactivity.[13–16]

Due to excellent osteogenic bioactivity for stimulating cell responses/bone tissues growth, tantalum (Ta) is considered as one of the most promising biomaterials for dental and orthopedic applications (such as artificial joints, cranioplasty plates, and porous structures for bone repair).[17] A thin layer of tantalum pentoxide (Ta_2O_5) naturally formed on a Ta surface plays crucial roles on its outstanding corrosion resistance, biocompatibility, and bioactivity.[18] Therefore, tantalum pentoxide (TP) coating was fabricated on Ti surface, which exhibited wonderful biocompatibility, bioactivity, and osseointegration.[19] TP coating was also prepared on the Ta surface that possessed admirable characteristics of good adherence and low modulus of elasticity compared with Ta substrate.[20] TP has been incorporated into the hydroxyapatite and bioglass to improve bioactivity and mechanical strengths.[21] Therefore, the noteworthy attributes of TP (eg, outstanding biocompatibility, bioactivity, and corrosion resistance as well as high hydrophilicity) exhibited its advantages for bone regeneration.[22]

As a dental implant in vivo, it should be closely combined with not only bone tissue to obtain osseointegration but also gingival tissue to achieve bio-sealing.[1,2] The achievement of bio-sealing of gingival tissue with dental implants can prevent bacterial invasion, which could avoid the occurrence of peri-implantitis and protect osseointegration.[2,23] Surface nanotopography of biomaterials plays key roles in regulating the cell/tissue responses, and biomaterials with surface nanostructure could provide the cells with binding sites, which were good for cell adhesion, spreading, and growth.[24,25] Therefore, creating a nanostructured surface on biomaterial would have great potential to improve the cell/tissue responses, and thereby promote tissue regeneration in vivo.

Consequently, in the present study, to endow PEEK surface with bioactivity for dental applications, TP coating was deposited on PEEK surface by utilizing vacuum evaporation (VE). The purpose of this work was to develop bioactive TP coating on PEEK surface to induce responses of rat bone marrow mesenchymal stem (RBMS) cells for bone regeneration and human gingival epithelial (HGE) cells for gingival regeneration that could achieve both osseointegration and bio-sealing for success of dental implant. We supposed that TP coating on PEEK could activate the responses of both RBMS cells and HGE cells. To test this hypothesis, the responses of RBMS cells (attachment, proliferation, and osteogenic differentiation) as well as HGE cells (attachment and proliferation) to TP coating of PEEK were studied in vitro.

Materials and Methods

Preparation and Characterization of TP Coating on PEEK

The specimens of PEEK (2 mm in thickness and 6 inches in diameter) were obtained from Victrex (450 G, Victrex, UK). TP coating on the PEEK surface was fabricated in vacuum coating equipment (OTFC-900, OPTORUN Co., Ltd, Japan). Typical parameters of vacuum coating process: evaporator source was Ta_2O_5 (degree of purity of 99%), working vacuum degree was 2×10^{-2} Pa, total power of the equipment was 80 KVA, working temperature was 100°C, the reaction gas is of high purity oxygen (O_2) and argon (Ar), the deposition rate was 18 nm/min and deposition time was 20 minutes. The specimens of PEEK with TP coating (PKTP) and PEEK without coating (used as controls) were cut into pieces (size of 10×10×2 mm),

which were cleaned with ethanol solution as well as deionized water 3-times, and dried at 70°C.

The surface morphology of the specimens (PEEK and PKTP), and cross-section morphology of PKTP were characterized by field-emission scanning electron microscopy (FESEM, S-4800, Hitachi Co., Japan). The element distributions of the specimens were characterized by utilizing energy dispersive spectrometry (EDS, S-4800, Hitachi Co., Japan) and X-ray photoelectron spectroscopy (XPS, ESCALAB 250Xi, Thermo Fisher Co., UK). In addition, the compositions and structures of specimens were analyzed by Fourier Transform Infrared Spectrometry (FTIR, Nicolet 6700, Nicolet Co., USA) and X-ray diffraction (XRD, 18KW/D/max2550VB/PC, Rigaku Co., Japan) with Cu-Kα source at 40 kV and 100 mA.

Roughness and Binding Strength of TP Coating

3D surface morphology as well as surface roughness of Ra (arithmetical mean deviation) of specimens (PEEK and PKTP) were investigated by utilizing atomic force microscopy (AFM, Multimode8, Bruker, Germany). The adhesion property of the coating to substrates was determined by scratch technique. For PKTP, the binding strength of the TP coating on PEEK was tested by Revetest® Scratch Tester (ST, Anton Paar Co., Austria). A standard conical Rockwell diamond spherical indenter (radius 100 μm) was utilized as a scratch counterpart to move across the PKTP surface with a linearly increasing normal load (Fn=0.01 N~20 N, speed was 5 N/s) at a constant speed (4 mm/min) with a length of total scratch of 2 mm. The scratches were determined by using an optical microscope of scratch platform to evaluate failure of the coating associated with the load.

Hydrophilicity, Surface Energy, and Protein Adsorption

The contact angles of water and diiodomethane of PEEK and PKTP were determined by utilizing a contact angle measurement (JC2000D2, Shanghai Zhongchen Digital Technology Equipment Co., Ltd., China). The surface energies of PEEK and PKTP were calculated according to Owen-Wendt theoretical formula.[23] Adsorption of protein on PEEK and PKTP was evaluated by using BSA. The specimens were placed into a 48-well cultured plate with BSA-PBS (1 mL, 10 μg/mL) solution (Shanghai Yuejin Medical Devices Co., Ltd., China) for 2 hours (37°C). The specimens were washed by utilizing deionized water 3-times to remove the unadsorbed proteins. After that, sodium dodecyl sulfate solution (Shanghai Yuanmu Biological Technology Co., Ltd., China) (2%, 0.5 mL) was added into detaching proteins from the specimen surface and the eluate was collected. Then the protein concentration in the eluate was evaluated by utilizing bicinchoninic acid assay (Beijing Solarbio Science & Technology Co., Ltd., China) through BCA Protein Assay Kit (Pierce Co., USA). The absorbance at 562 nm was tested by utilizing a microplate reader (Varioskan Flash, Thermo Scientific Co., USA) to get the protein adsorption amounts on the specimens.

Responses of RBMS Cells to TP Coating in vitro

The RBMS cells were isolated from femurs of 1-month-old male Sprague-Dawley rats (Laboratory Animal Center, Shanghai Ninth People's Hospital, School of Medicine, Shanghai Jiaotong University, China), which were applied to evaluate cells responses to the specimens (PEEK and PKTP). All animal procedures were approved by the Animal Care and Experiment Committee of Shanghai Ninth People's Hospital affiliated to Shanghai Jiaotong University (Shanghai, China), and the National Institutes of Health guidelines for the Care and Use of Laboratory Animals (NIH Publication No. 85–23, revised 1985) was followed. The RBMS cells were cultured in α-Modified Eagle Medium supplemented with fetal bovine serum (10%) and 1% double antibodies (streptomycin/penicillin) with CO_2 (5%) at 37°C. The specimens were co-cultured with the RBMS cells from passages 3–5. Before the cell experiments, the specimens were sterilized by utilizing ethyl alcohol (75%) for 30 minutes and then washed with PBS three times.

Morphology of RBMS Cells on TP Coating

The specimens were placed into a 24-well cell plate. The RBMS cells (density of 2×10^4 cells per well) were then seeded on the specimens. At 6, 12, and 24 hours after culturing, the liquid in the plate was removed and the specimens were washed with PBS. According to the manufacturer's instruction, the cell adhesion was quantitatively assessed by CyQUANT® assay kit (Life Technologies Co., USA). The cells (2×10^4 cells/well) were seeded on the specimens, and after cultured for 1, 3, and 5 days, the specimens with cells were washed by using PBS and fixed with glutaraldehyde (2.5 v%) for 24 hours at 4°C. After that, the cells were dehydrated with ethanol (10%, 30%, 50%, 70%, 85%, 90%, and 100%) for 8 minutes each time, and then dried at room

temperature. The cell morphology on the specimens was investigated with scanning electron microscopy (S-3400, Hitachi Co., Japan). Moreover, at 1, 3, and 5 days after culturing, the cells on the specimens were stained with FITC-phalloidin isothiocyanate (Sigma-Aldrich Co., China) as well as 4′,6-Diamidino-2-phenylindole dihydrochloride (Sigma-Aldrich Co., China). The cell morphology of fluorescence images of stained cells was obtained with a confocal laser scanning microscope (A1R, Nikon Co., Japan) to observe.

Adhesion and Proliferation of RBMS Cells on TP Coating

The adhesion and proliferation of RBMS cells on the specimens were assessed by a cell counting kit-8 (Beyotime-Biotech Co., China) assay. The cultured medium with 2×10^4 cells was inoculated on the specimen. The culture plates were placed in an incubator for 6, 12, and 24 hours for adhesion, while the time point was 1, 3, and 7 days for proliferation. At specific cultured times, the cultured medium in the wells was moved away, and then the specimen was washed by utilizing PBS three times. Then a working solution of medium (400 μL) and cell counting kit-8 (40 μL) were added into the well, and then incubated for 3 hours. The supernatant was pipetted into a 96-well plate, and a microplate reader (Synergy HT, Bio-Tek Co., USA) was utilized to read optical density (OD) at 450 nm.

ALP Activity of RBMS Cells on TP Coating

Alkaline phosphatase (ALP) activity of the cells on the specimens was determined by ALP assay kit (Beyotime Biotechnology, China) according to manufacturer's instructions. BMS cells (2×10^4 cells/well) were seeded on the specimens in 24-well plates for 7, 10, and 14 days, and then the specimens were washed with PBS three times. After that, 500 μL Nonidet P-40 (1%, Sigma-Aldrich, China) solution was added into per well to get cell lysate. Then p-nitrophenyl phosphate (Sigma-Aldrich, China) was added, and then incubated for another 30 minutes. After the incubation, the reaction was stopped by utilizing NaOH aqueous solution (0.1 mol/L). A microplate reader (Varioskan Flash, Thermo Scientific, USA) was utilized to assess the OD values of the cells at 405 nm wavelength. BCA Protein Assay Kit was utilized to assess the total protein contents in the cell lysate. The ALP activity was defined as the OD value (405 nm)/total protein contents.

Osteogenesis Genes Expressions of RBMS Cells on TP Coating

The osteogenic related genes expressions were evaluated by real-time PCR. After the RBMS cells were cultured on specimens (1×10^5 cells/well) for 3, 7, and 14 days, according to the manufacturer's instructions, total RNA was isolated from the cells using Trizol reagent (Invitrogen Co., USA). Afterwards, 1 μg of total RNA was reversely transcribed into complementary DNA (cDNA) using PrimeScript First Strand cDNA Synthesis Kit (TaKaRa Co., Japan). Bio-Rad real-time PCR system (Bio-Rad Co., USA) was used to perform the real-time PCR analysis on markers of runt-related transcription factor 2 (Runx2), alkaline phosphatase (ALP), osteopontin (OPN), and osteocalcin (OCN). In addition, glyceraldehyde-3-phosphate dehydrogenase (GAPDH) was used as the house-keeping gene for normalization. The forward and reverse primer sequences for the selected genes are listed in Table 1.

Responses of HGE Cells to TP Coating

Cells responses to specimens were determined by using HGE cells, which were obtained from the School of Medicine, Shanghai Jiaotong University, China. The HGE cells were cultured in Dulbecco's modified eagle medium (Shanghai XP Biomed Co., Ltd., China) with CO_2 (5%) at 37°C. The cultured mediums were supplemented with fetal bovine serum (10%) from Shanghai XP Biomed Co., Ltd., China, and double antibiotics (1%) containing penicillin and streptomycin.

Table 1 Primers Used for RT-PCR Analysis

Gene	Forward Primer Sequence (5′-3′)	Reverse Primer Sequence (5′-3′)
Runx2	ACTTCCTGTGCTCGGTGCT	GACGGTTATGGTCAAGGTGAA
ALP	ACCATTCCCACGTCTTCACATTT	AGACATTCTCTCGTTCACCGCC
OPN	GAGACCGTCTGAAACAGCGT	AACCACTGCCAGTCTCATGG
OCN	CCTCACACTCCTCGCCCTATT	CCCTCCTGCTTGGACACAAA
GAPDH	TGTTCCTACCCCCAATGTATCCG	TGCTTCACCACCTTCTTGATGTCAT

Abbreviations: RT-PCR, reverse transcription-polymerase chain reaction; Runx2, runt-related transcription factor 2; ALP, alkaline phosphatase; OPN, osteopontin; OCN, osteocalcin; GAPDH, glyceraldehyde-3-phosphate dehydrogenase.

Morphology of HGE Cells on TP Coating

The specimens were firstly sterilized by using high-temperature autoclave. Briefly, HGE cells (2×10^4 cells/well) were seeded on the specimens in 24-well plates. At 1 and 3 days after culturing, the specimens were washed by using PBS three times and maintained in glutaraldehyde solution (2.5%) for 2 hours. The specimens with the cells were stained with fluorescein isothiocyanate phalloidin (Sigma-Aldrich Co., China) for 30 minutes, then stained with 2-(4-amino-phenyl)-6-indoleformamide dihydrochloride (Sigma-Aldrich Co., China) for 10 minutes. The cell morphology was observed by confocal laser scanning microscope (CLSM, A1R, Nikon Co., Japan). Furthermore, the specimens with cells were dehydrated with various concentrations (10%, 30%, 50%, 70%, 85%, 90%, and 100%) of ethanol for 15 minutes. The cell morphology was observed by SEM.

Adhesion and Proliferation of HGE Cells on TP Coating

The cell counting kit-8 (Beyotime-Biotech Co., China) assay was used to determine adhesion as well as proliferation of HGE cells on the specimens. The cultured medium with 2×10^4 cells was inoculated on the specimens. The cell cultured plates were placed in an incubator for 6, 12, and 24 hours for cell adhesion, while the incubation time point was 1, 3, and 7 days for cell proliferation. At specific time points, the medium in the wells was moved away, and the specimen was washed by using PBS three times. After that, a working solution of medium (400 μL) and cell counting kit-8 (40 μL) were added into the well, and then incubated for 3 hours. The supernatant was pipetted into a 96-well plate, and optical density (OD) was read at 450 nm by utilizing a microplate reader (Synergy HT, Bio-Tek Co., USA).

Statistical Analysis

The clearance related to statistical analysis was applied to all the experiments by one-way analysis of variance (ANOVA) followed by Tukey's test, and all values were expressed as mean±standard deviations (SD). $P<0.05$ represented the differences, which were regarded as statistically significant.

Results

Characterization of TP Coating

From the photos of the specimens, in comparison with PEEK (Figure 1A), the surface of TP coating on PKTP (Figure 1E) slightly became dark. Figures 1(B, C, F, and G) revealed the EDS of element distribution maps of PEEK and PKTP. No Ta signal was seen on PEEK surface (Figure 1C). However, many red (Ta signals, Figure 1G) dots were seen on PKTP surface. Moreover, Figures 1(D and H) revealed the EDS spectrum of PEEK and PKTP. The C and O peaks were seen on the PEEK surface (Figure 1D) while Ta peaks appeared on the PKTP (Figure 1H). Figure 2 showed the SEM images of surface morphology of PEEK (Figure 2A and D) and PKTP (Figure 2B and E). The PEEK surface was smooth, and no particle was seen under different magnification. However, the PKTP surface was rough (Figure 2B). Under high

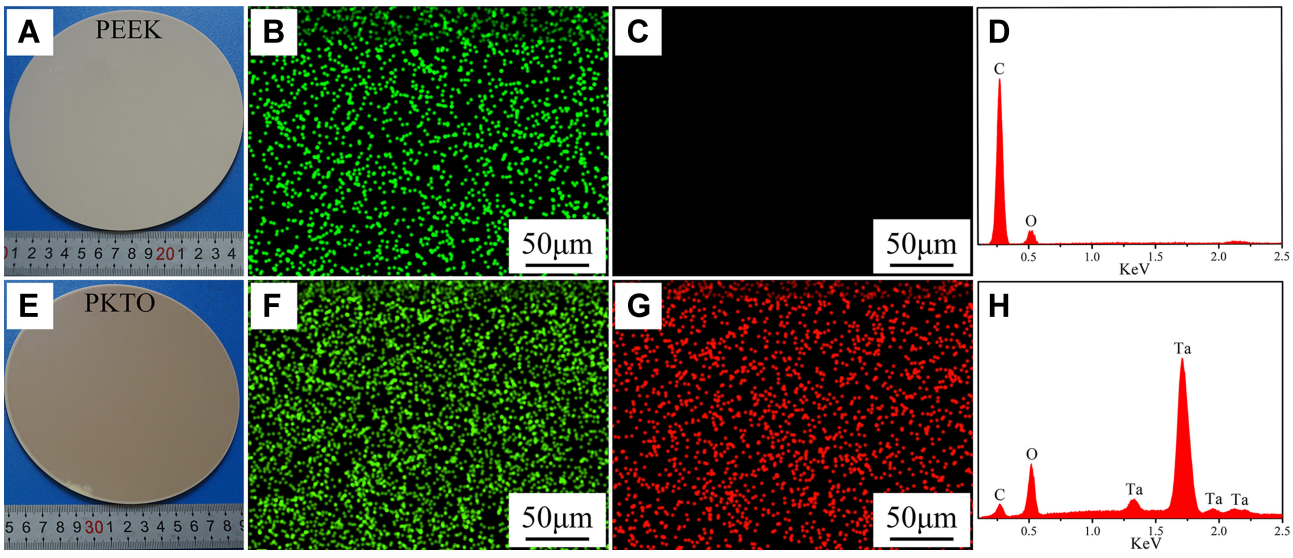

Figure 1 Digital photos of PEEK (**A**) and PKTP (**E**), and EDS of element distribution maps (**B, C, F, G**) of O (**B, F**) and Ta (**G**) and EDS spectra (**D, H**) of PEEK (**D**) and PKTP (**H**); and green dots (**B, F**) represent O signals and red dots (**G**) represent Ta signals.

Abbreviations: PEEK, polyetheretherketone; PKTP, polyetheretherketone with tantalum pentoxide coating; EDS, energy dispersive spectrometry; O, oxygen; Ta, tantalum.

magnification, the surface of PKTP contained many irregular bulges with a size of 10 nm (Figure 2E). Additionally, Figures 2(C and F) revealed the cross-sectional morphology of PKTP. The TP coating with a thickness of about 400 nm was dense, which was tightly bonded with PEEK substrate.

Figure 3A was the FTIR patterns of PEEK and PKTP. For PEEK, the peaks of diphenylketone bands appeared at 1650 cm^{-1}, 1490 cm^{-1}, and 925 cm^{-1}, the peak band of C=C in the benzene ring was found at 1600 cm^{-1}, and the peaks of C-O-C stretching vibration of diaryl groups were seen at 1158 cm^{-1} and 1190 cm^{-1}.[26] For PKTP, an apparent absorb peak appeared at 3304 cm^{-1} was attributed to the telescopic vibration peak of Ta hydroxyl group (Ta-OH), and the peak around 687 cm^{-1} belonged to the characteristic peak of TP. Figure 3B illustrated the XRD patterns of PEEK and PKTP. No characteristic peak of TP appeared in the XRD of PKTP in comparison with PEEK, indicating that the coating was non-crystalline TP (amorphous state). The XPS spectrum of PKTP was revealed in Figure 3C, and the signals of O, C, and Ta elements were seen. The Ta4f core-level XPS spectrum of PKTP (Figure 3D) was curve-fitted into two peaks with the binding energies of 25.6 eV and 27.5 eV, which were due to the Ta oxygen group (Ta-O) on the PKTP surface. The quantitative analysis of atom percentage of TP coating by XPS showed that the atom percentages of Ta and O were 28.17 at% and 39.21 at%. As a result, the atom ratio of Ta to O was 0.72, which was closed to the stoichiometric Ta_2O_5, confirming that the TP coating was stoichiometric Ta_2O_5. The FTIR and XPS revealed that the TP coating was deposited on PEEK.

Roughness and Bonding Strength of TP Coating

Figure 4 shows the AFM images of surface morphology of PEEK (Figure 4A) and PKTP (Figure 4B). The surface of PKTP was much rougher than PEEK. Furthermore, the surface roughness of PEEK and PKTP were 12.7±0.7 nm and 22.5±0.9 nm, as shown in Figure 4C. The load on delamination of TP coating was defined as the binding strength between coating and PEEK. The lower critical load (Lc1) indicated crack initiation of the coating while the higher critical load (Lc2) showed failure of the coating, which reflected the bonding strength of TP coating. As shown in Figure 4D, Lc1 and Lc2 of PKTP were 0.26 N and 1.08 N. Figure 4(E) was optical images of the scratch on the TP coating.

Hydrophilicity, Surface Energy, and Protein Adsorption

Figure 5A revealed the contact angles of water and diiodomethane of the specimens. The water contact angle of PEEK and PKTP was 88.5±2.6° and 70.5±4.1°, revealing that the hydrophilicity of PKTP with TP coating significantly increased compared with PEEK. Moreover, the

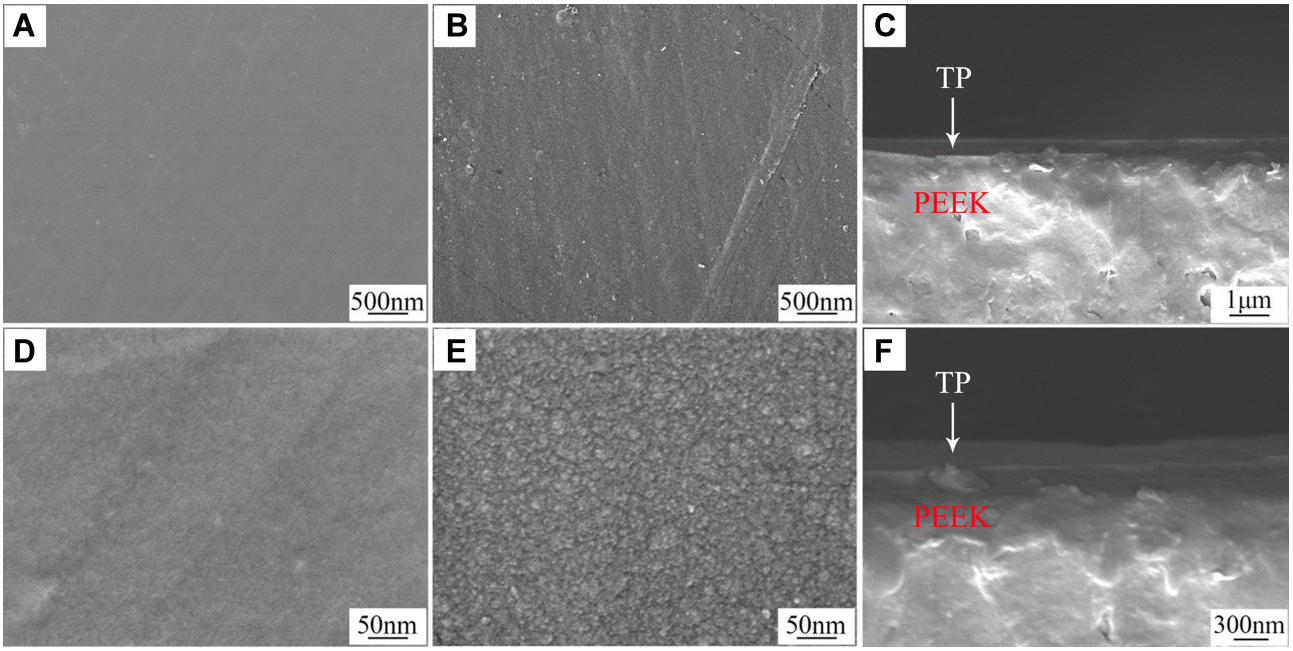

Figure 2 SEM images of surface morphologies of PEEK (**A, D**) and PKTP (**B, E**), and cross-section morphologies of PKTP for TP coating (**C, F**) under different magnifications.

Abbreviations: SEM, scanning electron microscopy; PEEK, polyetheretherketone; PKTP, polyetheretherketone with tantalum pentoxide coating; TP, tantalum pentoxide.

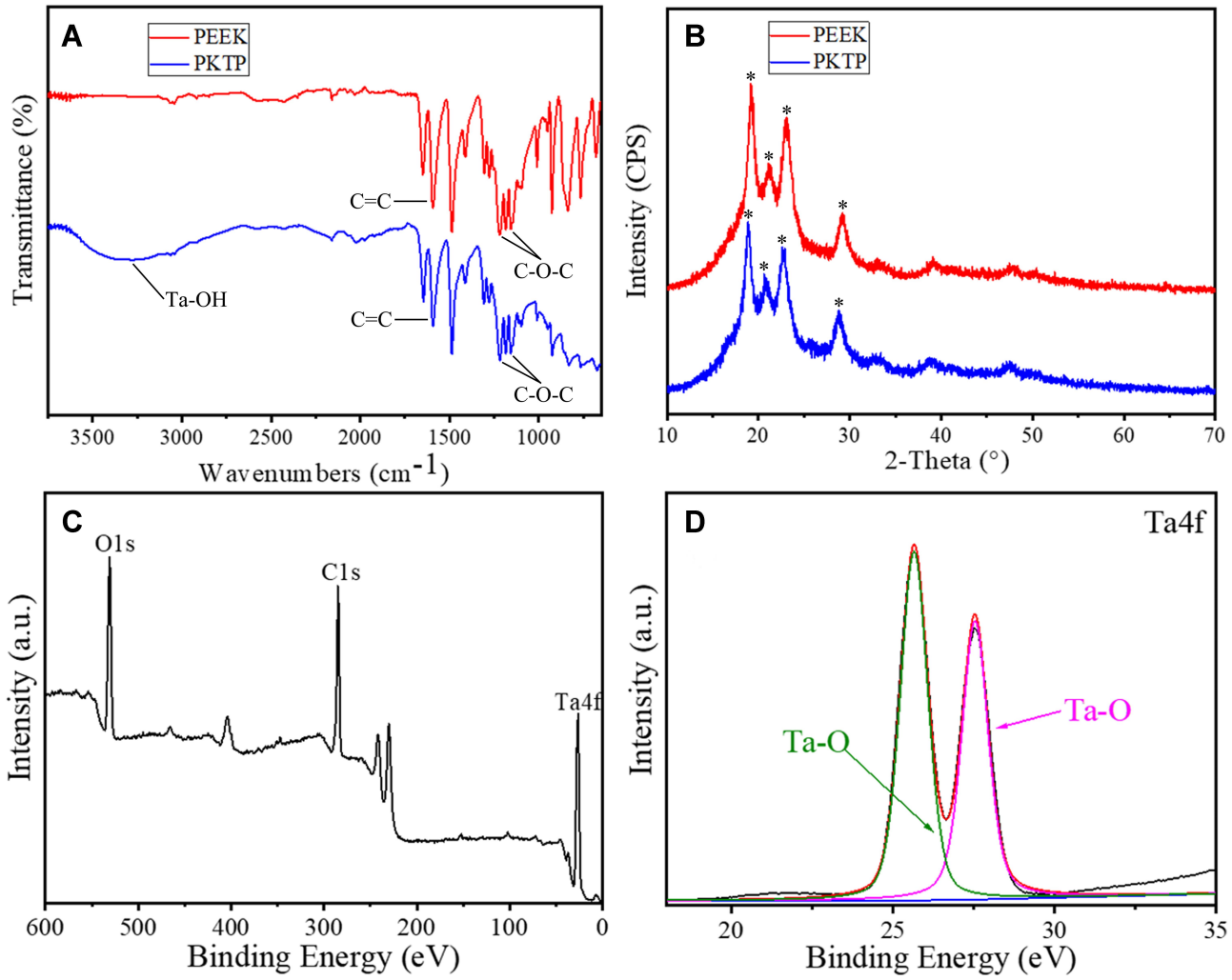

Figure 3 FTIR (**A**) and XRD (**B**) patterns of PEEK and PKTP, and wide-scan XPS spectrum (**C**) and N1s core-level XPS spectrum (**D**) of PKTP (*Represent the XRD peaks of PEEK).
Abbreviations: FTIR, Fourier transform infrared spectrometry; XRD, X-ray diffraction; PEEK, polyetheretherketone; PKTP, polyetheretherketone with tantalum pentoxide coating; XPS, X-ray photoelectron spectroscopy.

diiodomethane contact angle (Figure 5B) of PEEK and PKTP was 59.0±2.9° and 50.5±4.1°. Furthermore, Figure 5C was the surface energy of the specimens. The surface energy of PEEK and PKTP was 29.7±2.3 mJ/m^2 and 38.7±2.9 mJ/m^2. Figure 5D exhibited the adsorption of protein on specimens after being soaked into BSA-PBS solution for 2 hours. The adsorption of protein on PEEK and PKTP was 0.062±0.013 μg/mm^2 and 0.180±0.012 μg/mm^2.

Cells Responses to TP Coating in vitro

Morphology of RBMS Cells on Specimens

Figure 6 was the SEM images of morphology of RBMS cells on PEEK and PKTP at different times after culturing. At day 1, sparse cells with round morphology (no spreading) were seen on PEEK while the cells with obvious pseudopods were seen to spread on PKTP. At days 3 and 5, more cells with more filopodia were seen to attach and spread on the PKTP surface than PEEK. Apparently, the attachment and spreading of cells on PKTP was much better than PEEK. The CLSM images of RBMS cells on PEEK and PKTP at different time after culturing were shown in Figure 7. At days 1 and 3, sparse cells with round morphology (no spreading) were seen on PEEK surface while more cells with prominent pseudopods were seen to attach and spread on the PKTP surface. At day 5, more cells with more filopodia were seen on PKTP than PEEK. Apparently, the cell attachment and spreading on the PKTP surface were much better than PEEK.

Attachment, Proliferation and ALP Activity of RBMS Cells

Figure 8A was the attachment ratio of RBMS cells on the specimens at 6, 12, and 24 hours. The attachment ratio of cells

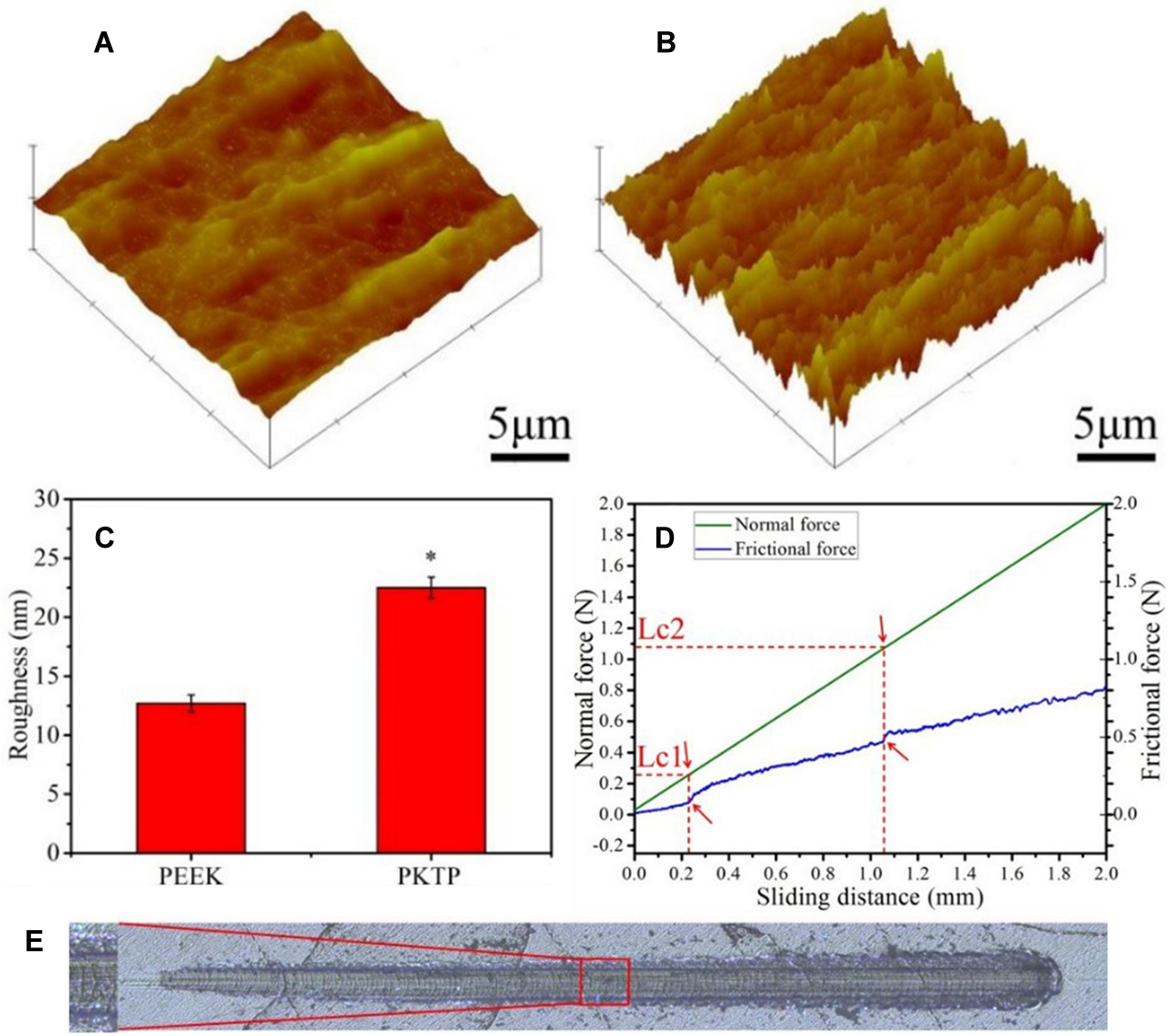

Figure 4 AFM images (**A, B**) and roughness (**C**) of PEEK (**A**) and PKTP (**B**) (*P<0.05, vs. PEEK), Frictional force–normal force curves (**D**) and optical microscopic images of the scratch (**E**) of PKTP.

Abbreviations: AFM, atomic force microscopy; PEEK, polyetheretherketone; PKTP, polyetheretherketone with tantalum pentoxide coating.

on PKTP increased with time while there was a slight increase for PEEK from 6 to 24 hours. Moreover, the attachment ratio of cells on PKTP were remarkably higher than PEEK. Figure 8B was the proliferation (expressed by OD values) of cells on the specimens at different times. The proliferation of cells on PKTP obviously increased with time while there was a slight increase for PEEK from day 1 to day 5. Moreover, the proliferation of cells on PKTP were significantly higher than PEEK. Figure 8C exhibited the ALP activity of cells on the specimens at 7, 10, and 14 days. The ALP activity of cells on PKTP obviously increased with time, while no significant increase was seen for PEEK. Furthermore, the ALP activity of cells on PKTP were remarkably higher than PEEK.

Osteogenic Genes Expressions of RBMS Cells

The expressions of osteogenic genes (Runx2, ALP, OPN, and OCN) of RBMS cells on PEKK and PKTP were shown in Figure 9. The genes expressions for PKTP increased with time while there was no significant increase for PEEK. At day 3, there were no obvious difference in the expression of Runx2, ALP, OPN, and OCN for both PEEK and PKTP. At days 7 and 14, the expressions of Runx2, ALP, OPN, and OCN for PKTP were significantly higher than PEEK.

Morphology of HGE Cells on Samples

Figure 10 was the SEM images of HGE cells on the samples at day 3 after culturing. The attachment and

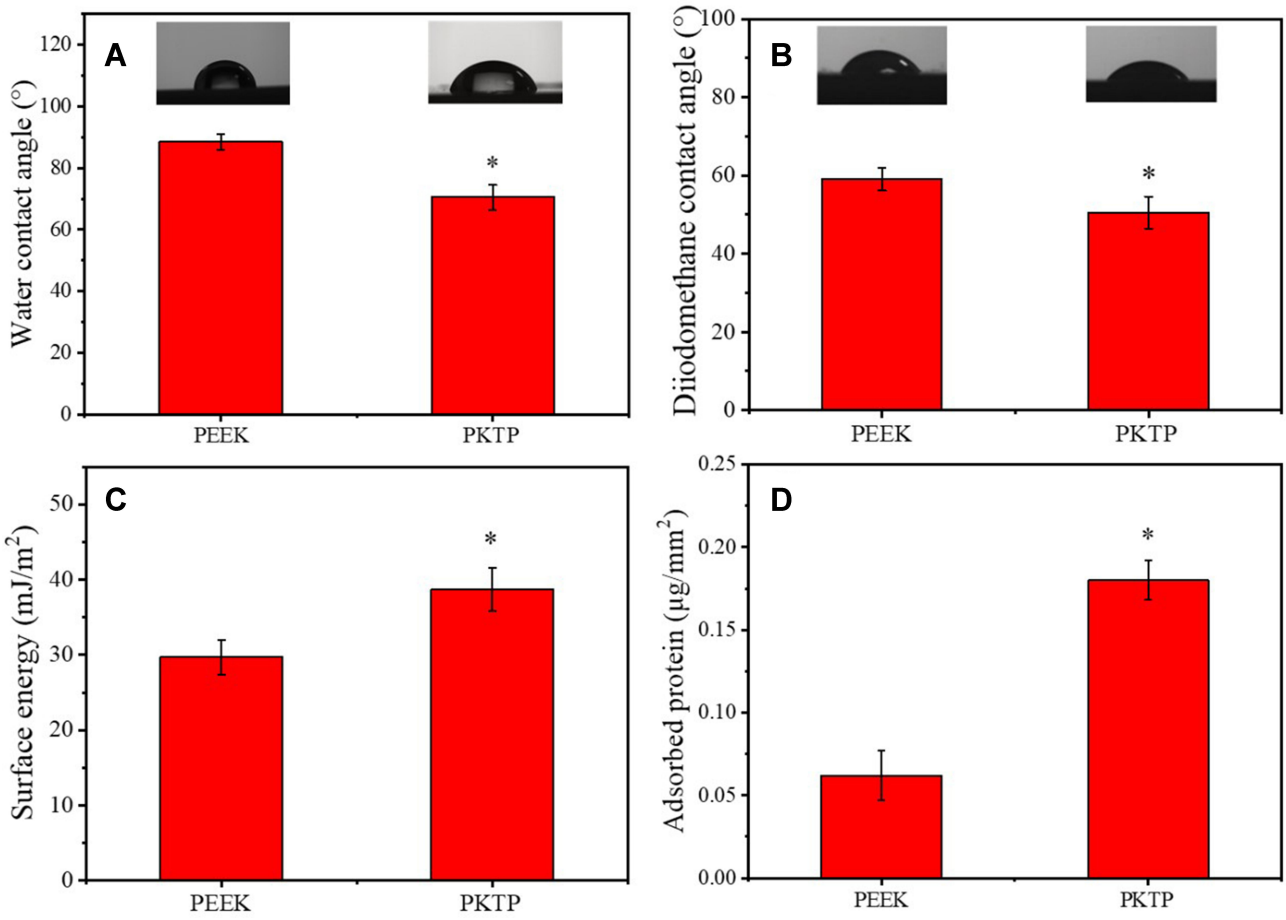

Figure 5 Water contact angle (**A**), diiodomethane contact angle (**B**), surface energy (**C**), and protein adsorption (**D**) of PEEK and PKTP (*P<0.05, vs PEEK).
Abbreviations: PEEK, polyetheretherketone; PKTP, polyetheretherketone with tantalum pentoxide coating.

spreading of the cells on PKTP were better than PEEK. In addition, more cells with numerous filopodia were seen on PKTP than PEEK. Figure 11 was the CLSM images of morphology of HGE cells on the samples at different times after culturing. It was seen that the number of the cells on PKTP obviously increased with time while there was a slight increase for PEEK at different times. Furthermore, more cells were observed on PKTP than PEEK.

Attachment and Proliferation of HGE Cells on Specimens

Figure 12A was the adhesion ratio of HGE cells on the specimens at different time after culturing. At 6, 12, and 24 hours, the adhesion ratio of cells on PKTP was significantly higher than PEEK. Figure 12B was the proliferation (expressed by OD values) of cells on the samples. It was seen that cell proliferation on PKTP obviously increased with time while only slightly increasing for PEEK. Moreover, the cell proliferation on PKTP were significantly higher than PEEK.

Discussion

Because of outstanding biocompatibility and mechanical strengths, PEEK has been widely used as biomedical implants for replacing bone tissue, which is also a promising implantable material for dental applications.[27] However, because of bioinert and hydrophobicity, PEEK does not induce adhesion, proliferation, differentiation, mineralization of osteoblasts, or promote bone regeneration both in vitro and in vivo.[28] Bioactive-coated PEEK implants have become a promising bone replacement material, which combines the advantage of both bioactive coating and PEEK.[29] In this study, to endow PEEK surface with bioactivity for tissue regeneration, TP was coated on PEEK (PKTP) by VE. The results showed that the dense TP coating of PKTP (thickness of around 400 nm) was stoichiometric TP, which was tightly bonded

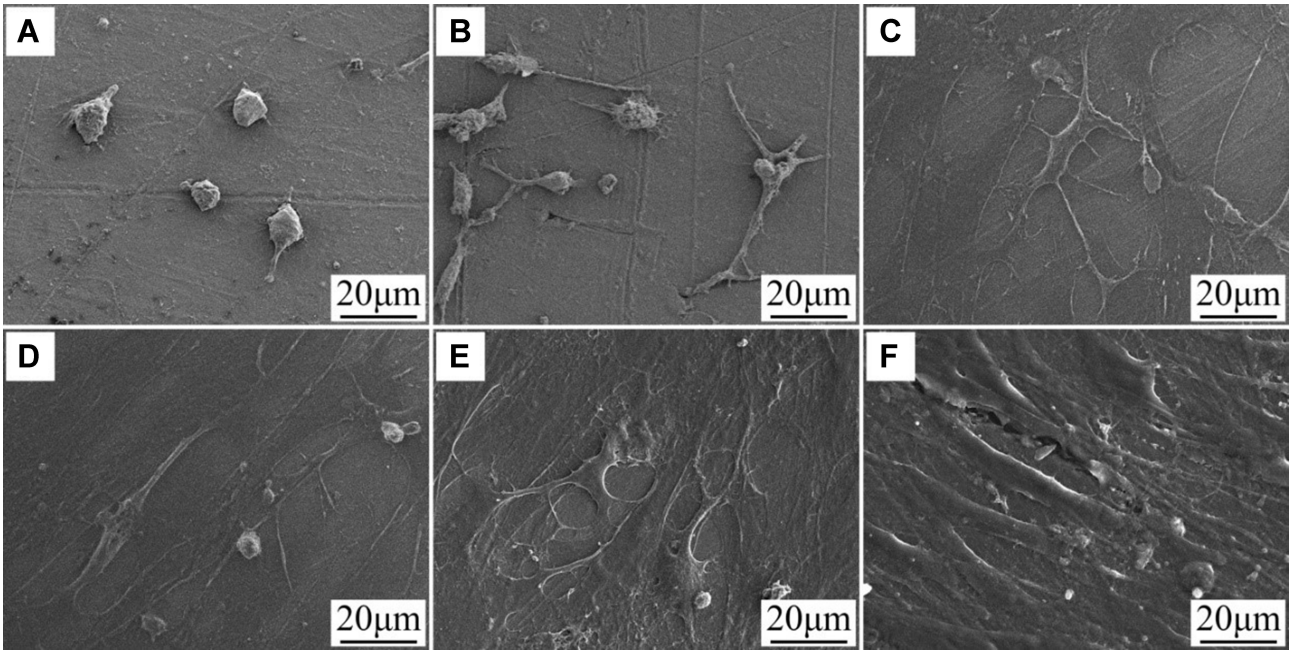

Figure 6 SEM images of morphology of RBMS cells on PEEK (**A–C**) and PKTP (**D–F**) at day 1 (**A, D**), 3 (**B, E**), and 5 (**C, F**) after culturing.
Abbreviations: SEM, scanning electron microscopy; RBMS, rat bone marrow mesenchymal stem; PEEK, polyetheretherketone; PKTP, polyetheretherketone with tantalum pentoxide coating.

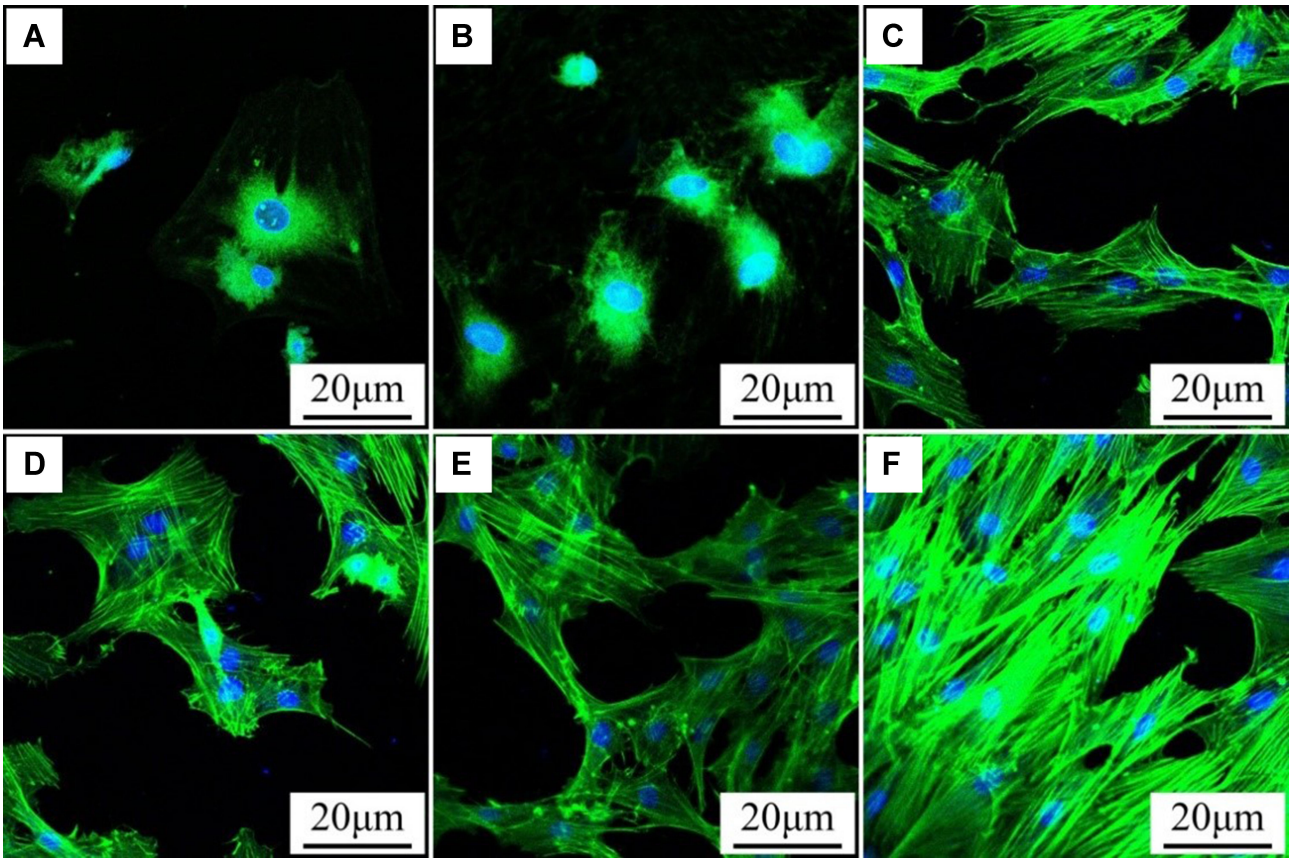

Figure 7 CLSM images of morphology of RBMS cells on PEEK (**A–C**) and PKTP (**D–F**) at day 1 (**A, D**), 3 (**B, E**) and 5 (**C, F**) after culturing.
Abbreviations: CLSM, confocal laser scanning microscope; RBMS, rat bone marrow mesenchymal stem; PEEK, polyetheretherketone; PKTP, polyetheretherketone with tantalum pentoxide coating.

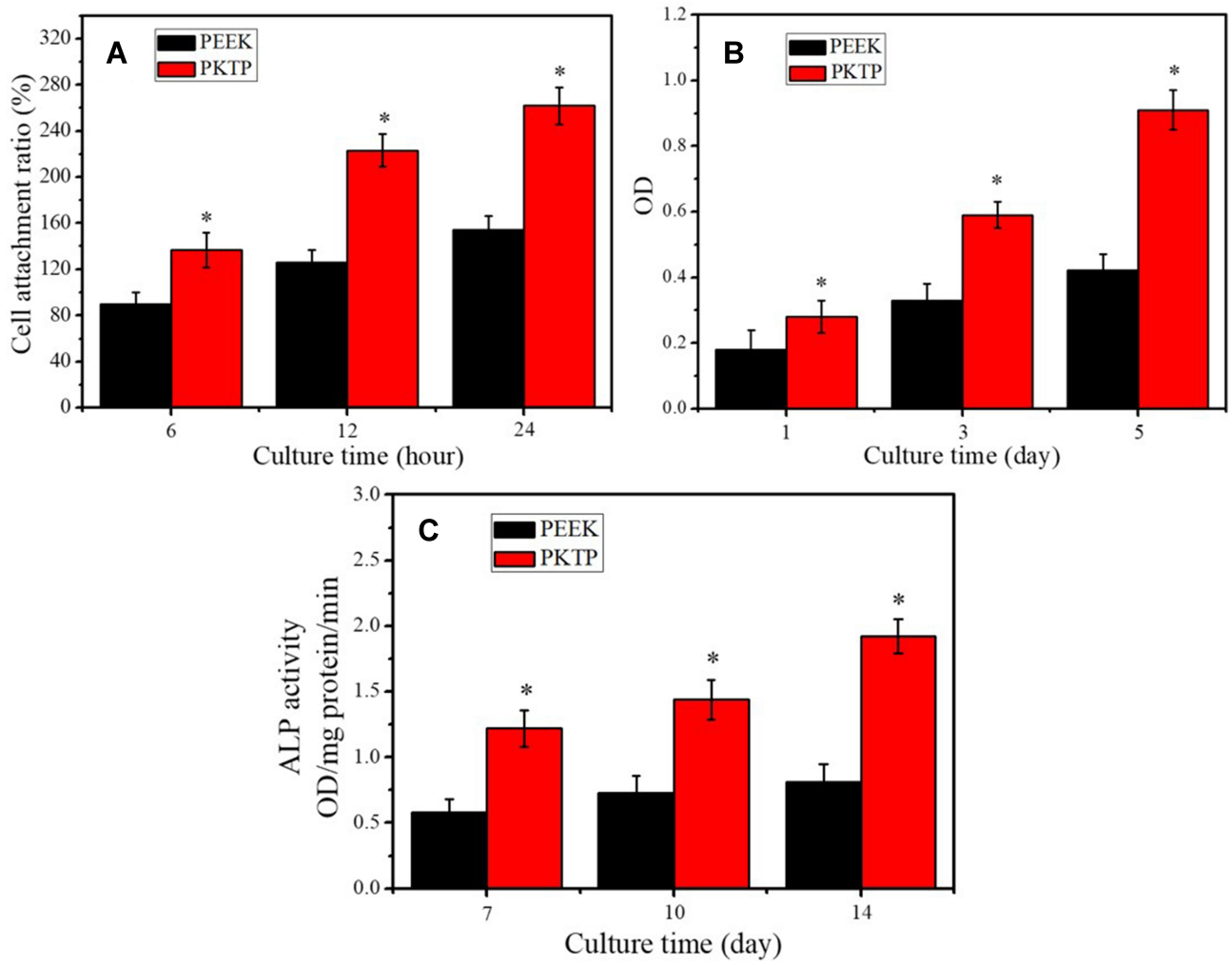

Figure 8 Attachment ratio (**A**), OD values (**B**) and ALP activity (**C**) of RBMS cells cultured on PEEK and PKTP for different time (*P<0.05, vs PEEK).
Abbreviations: OD, optical density; ALP, alkaline phosphatase; RBMS, rat bone marrow mesenchymal stem; PEEK, polyetheretherketone; PKTP, polyetheretherketone with tantalum pentoxide coating.

with PEEK. Furthermore, the coating of PKTP was non-crystalline TP, showing amorphous phase. PEEK revealed a smooth surface while PKTP exhibited a rough surface duo to the TP coating containing many irregular bulges with sizes of around 10 nm. Therefore, the coating of PKTP was nanostructured TP.

The surface features (eg, composition, micro-nano morphology, roughness, hydrophilicity) of dental materials have remarkable impacts on the responses of cells/tissues.[30,31] In the present study, the TP coating with nanostructure significantly improved the surface roughness of PKTP compared with PEEK. The increase of surface roughness of implants for inducing cell attachment was due to the improvement of surface-to-volume ratio that provided more sites for cell attachment.[32] Moreover, in comparison with PEEK, the hydrophilicity of PKTP obviously increased because of the hydrophilicity of TP as well as formation of the hydrophilic group of hydroxyl (-OH) on the TP coating.[33] Furthermore, compared with PEEK, the surface energy of PKTP obviously increased due to the TP with high surface energy. The adsorption of proteins was the initial pivotal step that affected the cell behaviors on the dental implant surface, because the cells sense the layer of adsorbed protein on the foreign surface.[34] The adsorption of proteins would alter the physico-chemical properties of the implant surface, and thereby inducing cellular response.[35] In this study, due to the TP coating, the adsorption of proteins on PKTP was obviously enhanced compared with PEEK. The adsorption of protein strongly depended on some surface factors such as chemical composition, nanostructure, and roughness as well as hydrophilicity.[36] Consequently, the enhancements of proteins adsorption on PKTP were due to not only the improved

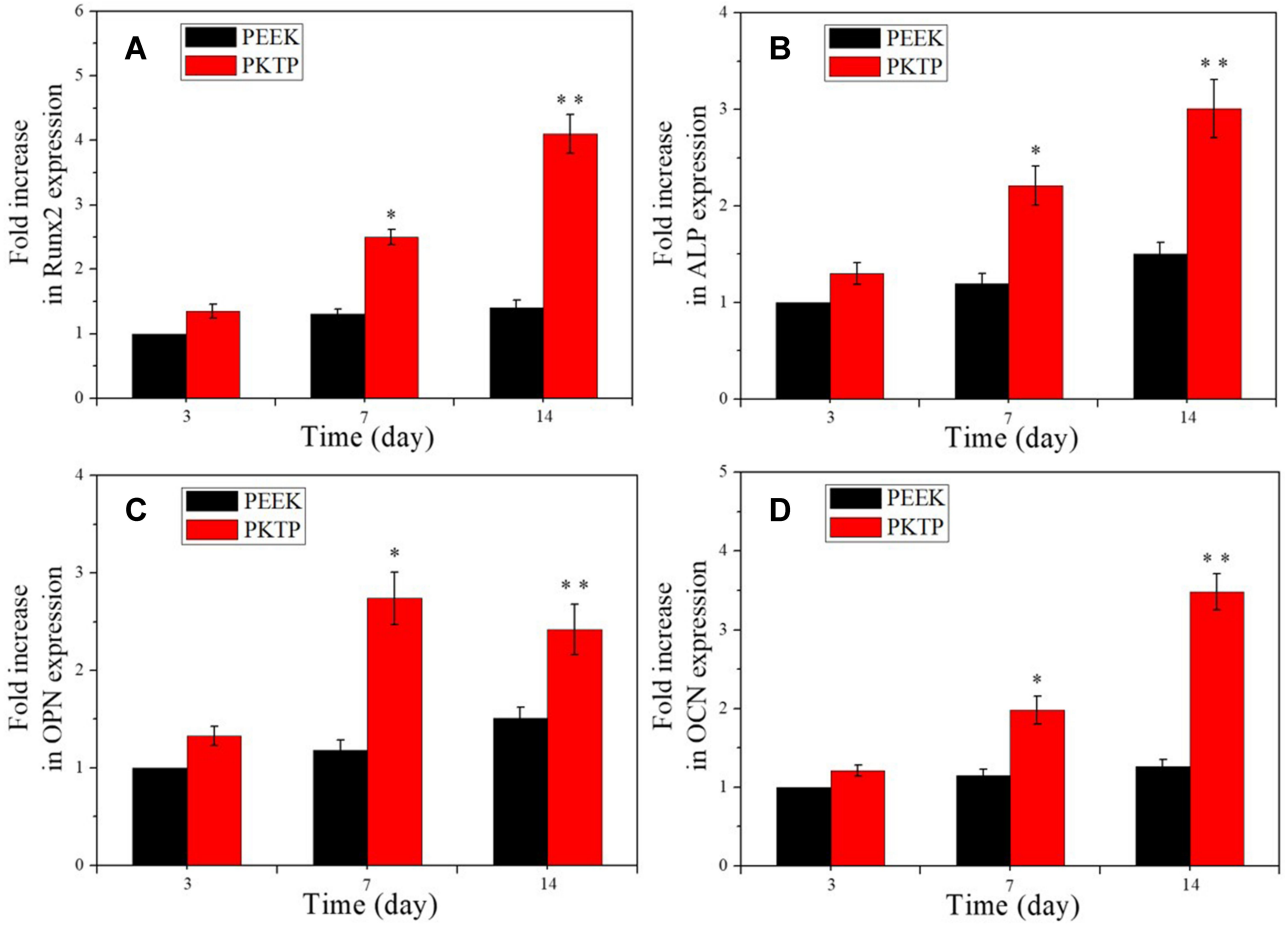

Figure 9 Expressions of osteogenic genes of Runx2 (**A**), ALP (**B**), OPN (**C**), and OCN (**D**) of RBMS cells on the specimens at different time after culturing (*P<0.05, **P<0.01, vs PEEK).

Abbreviations: Runx2, runt-related transcription factor 2; ALP, alkaline phosphatase; OPN, osteopontin; OCN, osteocalcin; RBMS, rat bone marrow mesenchymal stem; PEEK, polyetheretherketone.

roughness and hydrophilicity but also nanostructured surface of TP coating. The hydrophilic and rough surface with nanostructure of PKTP adsorbed more proteins, which might result in a favorable osteogenic microenvironment.[37]

The adhesion of cells mainly depended on surface performances (eg, topological structure, hydrophilicity) of dental implants.[33] During bone remodeling procedure, the proliferation of cells on the implants was the second key stage after cell adhesion, which determined the subsequent osteogenic differentiation of cells and new bone regeneration.[38] In this study, the RBMS cells adhesion on PKTP was remarkably higher than PEEK, and the cells revealed better spreading on PKTP in comparison with PEEK. Moreover, the proliferation of the RBMS cells on PKTP was obviously higher than PEEK. It could be suggested that the inducing of adhesion, spreading, and proliferation of cells on TP coating of PKTP were due to the improvements of surface performances (eg, roughness and hydrophilicity as well as adsorption of proteins) as well as the presence of nanostructured TP. ALP was generally regarded as a marker for early osteogenic differentiation, and the increase of ALP activity revealed the osteogenic differentiation of cells.[39] In the present study, the ALP activity of the cells on PKTP was remarkably higher than PEEK, indicating the TP coating of PKTP promoted osteogenic differentiation of RBMS cells. The expressions of osteogenic related genes (Runx2, ALP, OPN, and OCN) played key roles in the osteogenic differentiation of osteoblasts.[8,13] In this study, the expressions of Runx2, ALP, OPN, OCN, of RBMS cells on PKTP were significantly higher than PEEK. Consequently, the TP coating of PKTP remarkably stimulated expressions of osteogenic related genes, and thereby exciting osteogenic differentiation of the RBMS cells.

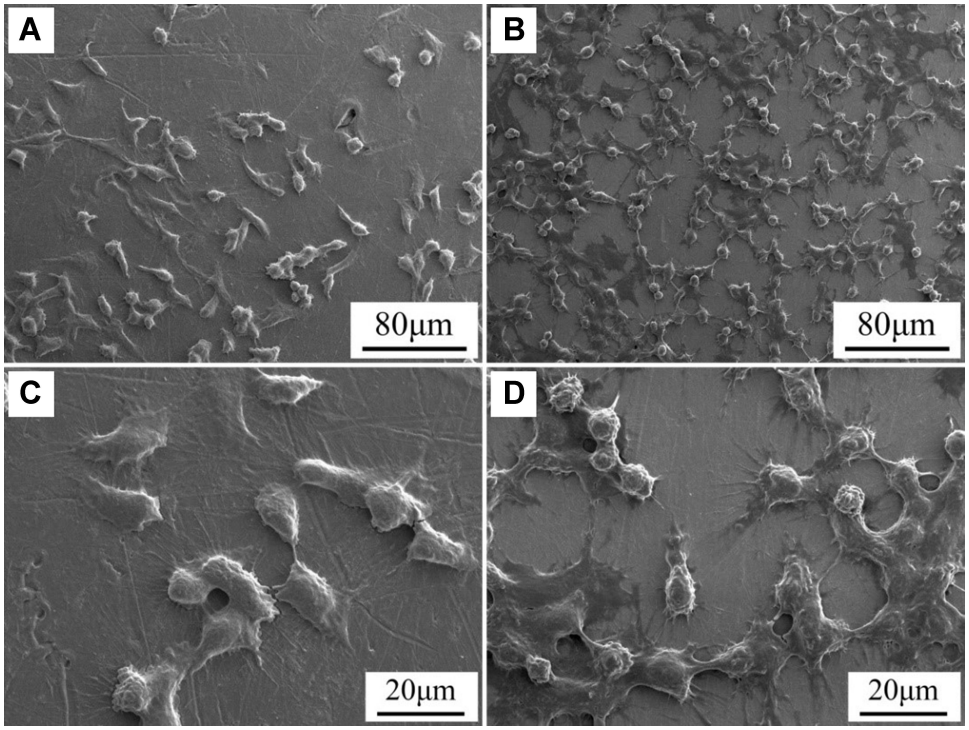

Figure 10 SEM images (under different magnifications) of morphology of HGE cells cultured on PEEK (**A, C**) and PKTP (**B, D**) for 3 days.
Abbreviations: SEM, scanning electron microscopy; HGE, human gingival epithelial; PEEK, polyetheretherketone; PKTP, polyetheretherketone with tantalum pentoxide coating.

The success of dental implants mainly depended on integration with not only bone tissue but also gingival tissue.[1,2] The gingival epithelium adhesion on the implant surface was the initial bio-barrier to prevent bacteria and metabolite, while the loss of gingival tissue adhesion on the implant surface was one of the most key reasons for the failure of implantation.[2,23] In the present study, compared with PEEK, the adhesion of HGE cells on PKTP significantly increased. Moreover, compared with PEEK, the proliferation of HGE cells on PKTP remarkably increased. As a result, the significant improvements of adhesion as well as proliferation of HGE cells on PKTP were due to the rough and hydrophilic PT coating with a nanostructured surface, which played significant roles in inducing the responses of HGE cells. We expected that PKTP with improved surface performances could stimulate the formation of bio-sealing at the interface of gingival tissue-implant.

The biological properties of dental implants were significantly influenced by the surface features, which might provide a favorable microenvironment for adsorption of proteins, and thereby affect the cell behaviors and functions.[40] In this study, compared with PEEK, the nanostructured TP coating on PEEK remarkably improved the surface performances of PKTP, which obviously induced the responses of both RBMS cells and HGE cells. Consequently, the significant enhancements of cellular responses of the two kinds of cells to PKTP were ascribed to the improved surface performances, which were the synergistic effects of several factors (eg, composition, nanostructure, roughness, hydrophilicity, and surface energy). The RBMS cells and HGE cells possess different physiological functions, the former will form bone tissue that achieves osteointegration for fixation of dental implants, while the latter will develop gingival tissue that obtains bio-sealing for preventing bacterial invasion and protecting osteointegration.[41] In short, PKTP with excellent cytocompatibility not only induced the responses (attachment and proliferation as well as differentiation) of RBMS cells but also stimulated the responses (attachment and proliferation) of HGE cells. Therefore, after being implanted in vivo, it is expected that PKTP as a dental implant could be integrated with not only bone tissue but also gingival tissue to achieve long-term stability. Thereby PKTP would be a promising candidate as a dental material for replace missing teeth.

Conclusions

In the present study, nanostructured coating of noncrystalline TP on PEEK surface was fabricated by VE. In comparison with PEEK, the surface roughness,

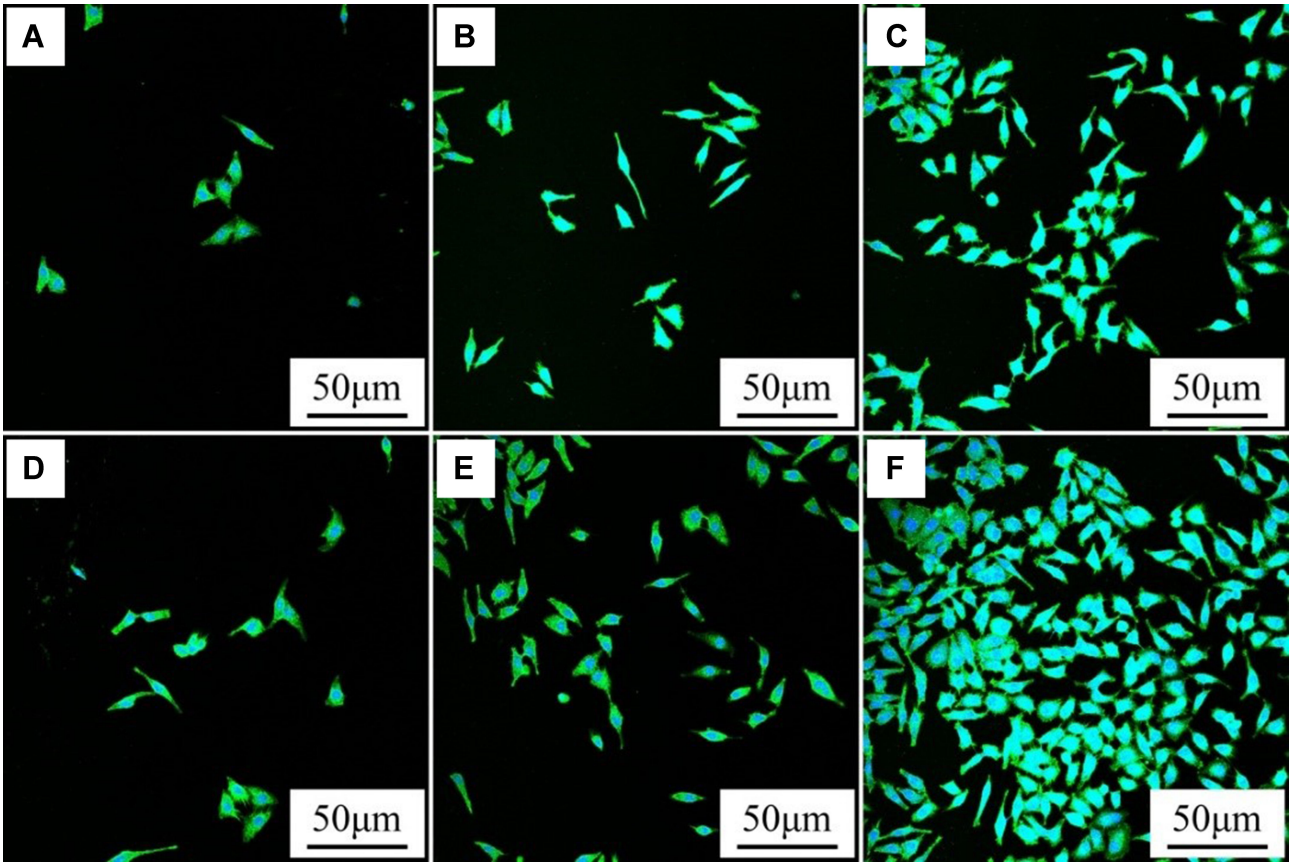

Figure 11 CLSM images of morphology of HGE cells on PEEK (**A–C**) and PKTP (**D–F**) at 12 (**A, D**), 24 (**B, E**), and 72 (**C, F**) hours after culturing.
Abbreviations: CLSM, confocal laser scanning microscope; HGE, human gingival epithelial; PEEK, polyetheretherketone; PKTP, polyetheretherketone with tantalum pentoxide coating.

hydrophilicity, and surface energy as well as protein adsorption of the TP coating of PKTP were remarkably increased. Furthermore, the responses (attachment, proliferation, and ALP activity as well as osteogenic gene expression) of RBMS cells and responses (attachment as well as proliferation) of HGE cells to PKTP were apparently enhanced in comparison with PEEK. Therefore, the nanostructured surface of TP coating on PEEK had

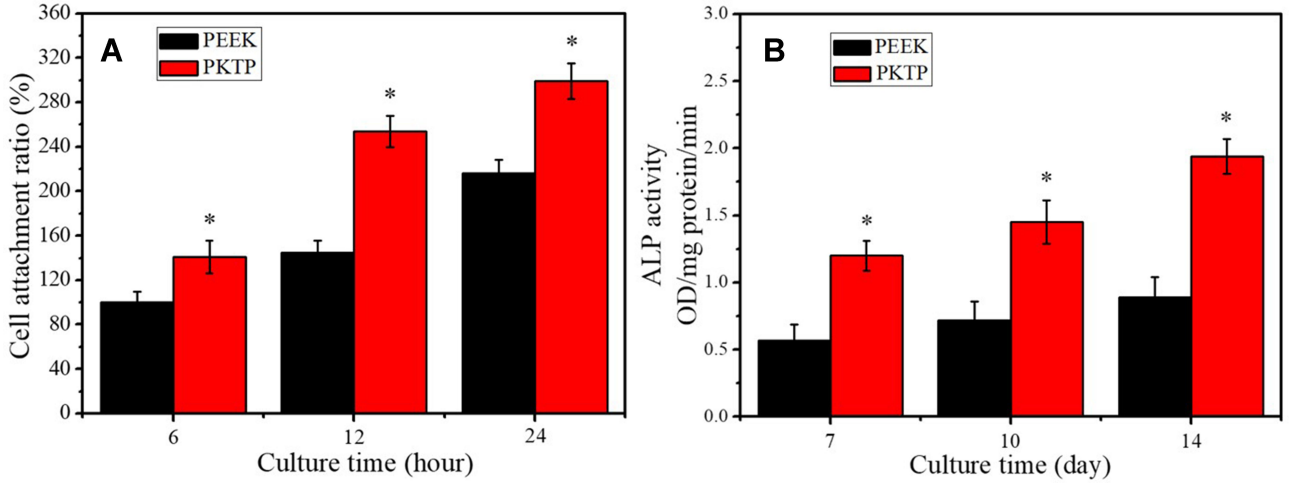

Figure 12 Attachment ratio (**A**) and OD values (**B**) of HGE cells cultured on PEEK and PKTP for different times (*P<0.05, vs PEEK).
Abbreviations: OD, optical density; HGE, human gingival epithelial; PEEK, polyetheretherketone; PKTP, polyetheretherketone with tantalum pentoxide coating.

apparent effects on the physical-chemical as well as biological properties of PKTP. In short, PKTP with TP coating with outstanding cytocompatibility and improved surface performances significantly induced the responses of both RBMS cells and HGE cells, thereby PKTP might be a potential candidate as a dental material for replacing missing teeth.

Acknowledgments

This work was supported by the Major Program of Development Fund for Shanghai Zhangjiang National Innovation Demonstration Zone "Stem Cell Strategic Biobank and Stem Cell Clinical Technology Transformation Platform" (ZJ2018-ZD-004).

Disclosure

The authors report no conflicts of interest in this work.

References

1. Esposito M, Worthington HV. Interventions for replacing missing teeth: dental implants in zygomatic bone for the rehabilitation of the severely deficient edentulous maxilla. *Cochrane Database Syst Rev*. 2013;9: UNSP CD004151. doi:10.1002/14651858.CD004151.pub3
2. Marin-Pareja N, Salvagni E, Guillem-Marti J, Aparicio C, Ginebra MP. Collagen-functionalised titanium surfaces for biological sealing of dental implants: effect of immobilisation process on fibroblasts response. *Colloid Surf B*. 2014;122:601–610. doi:10.1016/j.colsurfb.2014.07.038
3. Kaur M, Singh K. Review on titanium and titanium based alloys as biomaterials for orthopaedic applications. *Mat Sci Eng C-Mater*. 2019;102:844–862. doi:10.1016/j.msec.2019.04.064
4. Li YH, Yang C, Zhao HD, Qu SG, Li XQ, Li YY. New developments of Ti-based alloys for biomedical applications. *Materials*. 2014;7 (3):1709–1800. doi:10.3390/ma7031709
5. Stenlund P, Omar O, Brohede U, et al. Bone response to a novel Ti-Ta-Nb-Zr alloy. *Acta Biomater*. 2015;20:165–175. doi:10.1016/j.actbio.2015.03.038
6. Najeeb S, Zafar MS, Khurshid Z, Siddiqui F. Applications of polyetheretherketone (PEEK) in oral implantology and prosthodontics. *J Prosthodont Res*. 2016;60(1):12–19. doi:10.1016/j.jpor.2015.10.001
7. Kurtz SM, Devine JN. PEEK biomaterials in trauma, orthopedic, and spinal implants. *Biomaterials*. 2007;28(32):4845–4869. doi:10.1016/j.biomaterials.2007.07.013
8. Lu T, Wen J, Qian S, et al. Enhanced osteointegration on tantalum-implanted polyetheretherketone surface with bone-like elastic modulus. *Biomaterials*. 2015;51:173–183. doi:10.1016/j.biomaterials.2015.02.018
9. Panayotov IV, Orti V, Cuisinier F, Yachouh J. Polyetheretherketone (PEEK) for medical applications. *J Mater Sci Mater M*. 2016;27 (7):118. doi:10.1007/s10856-016-5731-4
10. Briem D, Strametz S, Schröoder K, et al. Response of primary fibroblasts and osteoblasts to plasma treated polyetheretherketone (PEEK) surfaces. *J Mater Sci Mater M*. 2005;16(7):671–677. doi:10.1007/s10856-005-2539-z
11. Poulsson AHC, Eglin D, Zeiter S, et al. Osseointegration of machined, injection moulded and oxygen plasma modified PEEK implants in a sheep model. *Biomaterials*. 2014;35(12):3717–3728. doi:10.1016/j.biomaterials.2013.12.056
12. Liu XY, Chu PK, Ding CX. Surface modification of titanium, titanium alloys, and related materials for biomedical applications. *Mater Sci Eng R*. 2004;47(3–4):49–121. doi:10.1016/j.mser.2004.11.001
13. Rasouli R, Barhoum A, Uludag H. A review of nanostructured surfaces and materials for dental implants: surface coating, patterning and functionalization for improved performance. *Biomater Sci*. 2018;6(6):1312–1338. doi:10.1016/j.mser.2004.11.001
14. Awaja F, Bax DV, Zhang SN, James N, McKenzie DR. Cell adhesion to PEEK treated by plasma immersion ion implantation and deposition for active medical implants. *Plasma Process Polym*. 2012;9 (4):355–362. doi:10.1002/ppap.201100034
15. Han CM, Lee EJ, Kim HE, et al. The electron beam deposition of titanium on polyetheretherketone (PEEK) and the resulting enhanced biological properties. *Biomaterials*. 2010;31(13):3465–3470. doi:10.1016/j.biomaterials.2009.12.030
16. Tsougeni K, Vourdas N, Tserepi A, Gogolides E, Cardinaud C. Mechanisms of oxygen plasma nanotexturing of organic polymer surfaces: from stable super hydrophilic to super hydrophobic surfaces. *Langmuir*. 2009;25(19):11748–11759. doi:10.1021/la901072z
17. Levine BR, Sporer S, Poggie RA, Della Valle CJ, Jacobs JJ. Experimental and clinical performance of porous tantalum in orthopedic surgery. *Biomaterials*. 2006;27(27):4671–4681. doi:10.1016/j.biomaterials.2006.04.041
18. Horandghadim N, Khalil-Allafi J, Urgen M. Influence of tantalum pentoxide secondary phase on surface features and mechanical properties of hydroxyapatite coating on NiTi alloy produced by electrophoretic deposition. *Surf Coat Technol*. 2020;386:125458. doi:10.1016/j.surfcoat.2020.125458
19. Sarraf M, Razak BA, Nasiri-Tabrizi B, et al. Nanomechanical properties, wear resistance and in-vitro characterization of Ta_2O_5 nanotubes coating on biomedical grade Ti-6Al-4V. *J Mech Behav Biomed*. 2017;66:159–171. doi:10.1016/j.jmbbm.2016.11.012
20. Wang N, Li HY, Wang JS, Chen S, Ma YP, Zhang ZT. Study on the anticorrosion, biocompatibility, and osteoinductivity of tantalum decorated with tantalum oxide nanotube array films. *ACS Appl Mater Inter*. 2012;4(9):4516–4523. doi:10.1021/am300727v
21. Horandghadim N, Khalil-Allafi J, Urgen M. Effect of Ta_2O_5 content on the osseointegration and cytotoxicity behaviors in hydroxyapatite-Ta_2O_5 coatings applied by EPD on superelastic NiTi alloys. *Mat Sci Eng C-Mater*. 2019;102:683–695. doi:10.1016/j.msec.2019.05.005
22. Sun YS, Chang JH, Huang HH. Corrosion resistance and biocompatibility of titanium surface coated with amorphous tantalum pentoxide. *Thin Solid Films*. 2013;528:130–135. doi:10.1016/j.tsf.2012.06.088
23. Chai WL, Brook IM, Palmquist A, van Noort R, Moharamzadeh K. The biological seal of the implant-soft tissue interface evaluated in a tissue-engineered oral mucosal model. *J R Soc Interface*. 2012;9 (77):3528–3538. doi:10.1098/rsif.2012.0507
24. Jo YK, Choi BH, Kim CS, Cha HJ. Diatom-inspired silica nanostructure coatings with controllable microroughness using an engineered mussel protein glue to accelerate bone growth on titanium-based implants. *Adv Mater*. 2017;29:1704906. doi:10.1002/adma.201704906
25. Souza JCM, Sordi MB, Kanazawa M, et al. Nano-scale modification of titanium implant surfaces to enhance osseointegration. *Acta Biomater*. 2019;94:112–131. doi:10.1016/j.actbio.2019.05.045
26. Liu XY, Choi HS, Park BR, Lee HK. Amphiphobicity of polyvinylidene fluoride porous films after atmospheric pressure plasma intermittent etching. *Appl Surf Sci*. 2011;257(21):8828–8835. doi:10.1016/j.apsusc.2011.04.069
27. Rosenthal G, Ng I, Moscovici S, et al. Polyetheretherketone implants for the repair of large cranial defects: a 3-center experience. *Neurosurgery*. 2014;75(5):523–529. doi:10.1227/NEU.0000000000000477
28. Ren YF, Sikder P, Lin BR, Bhaduri SB. Microwave assisted coating of bioactive amorphous magnesium phosphate (AMP) on polyetheretherketone (PEEK). *Mater Sci Eng C-Mater*. 2018;85:107–117. doi:10.1016/j.msec.2017.12.025

29. Mahjoubi H, Buck E, Manimunda P, et al. Surface phosphonation enhances hydroxyapatite coating adhesion on polyetheretherketone and its osseointegration potential. *Acta Biomater*. 2017;47:149–158. doi:10.1016/j.actbio.2016.10.004
30. Bello DG, Fouillen A, Badia A, Nanci A. A nanoporous titanium surface promotes the maturation of focal adhesions and formation of filopodia with distinctive nanoscale protrusions by osteogenic cells. *Acta Biomater*. 2017;60:339–349. doi:10.1016/j.actbio.2017.07.022
31. Sharifianjazi F, Pakseresht AH, Shahedi Asl M, et al. Hydroxyapatite consolidated by zirconia: applications for dental implant. *J Compos Compd*. 2020;2(2):26–34. doi:10.29252/jcc.2.1.4
32. Weng L, Webster TJ. Nanostructured magnesium has fewer detrimental effects on osteoblast function. *Int J Nanomed*. 2013;8:1773–1781. doi:10.2147/IJN.S39031
33. Wang WG, Luo CJ, Huang J, Edirisinghe M. PEEK surface modification by fast ambient-temperature sulfonation for bone implant applications. *J R Soc Interface*. 2019;16(152):20180955. doi:10.1098/rsif.2018.0955
34. Fenoglio I, Fubini B, Ghibaudi EM, Turci F. Multiple aspects of the interaction of biomacromolecules with inorganic surfaces. *Adv Drug Deliver Rev*. 2011;63(13):1186–1209. doi:10.1016/j.addr.2011.08.001
35. Huang R, Lu SM, Han Y. Role of grain size in the regulation of osteoblast response to Ti-25Nb-3Mo-3Zr-2Sn alloy. *Colloid Surf B*. 2013;111:232–241. doi:10.1016/j.colsurfb.2013.06.007
36. Cheng QW, Yuan B, Chen XN, et al. Regulation of surface micro/nano structure and composition of polyetheretherketone and their influence on the behavior of MC3T3-E1 pre-osteoblasts. *J Mater Chem B*. 2019;7(37):5713–5724. doi:10.1039/c9tb00943d
37. Schweikl H, Muller R, Englert C, et al. Proliferation of osteoblasts and fibroblasts on model surfaces of varying roughness and surface chemistry. *J Mater Sci Mater M*. 2007;18(10):1895–1905. doi:10.1007/s10856-007-3092-8
38. Wang LL, Lu GZ, Lu Q, Kaplan DL. Controlling cell behavior on silk nanofiber hydrogels with tunable anisotropic structures. *ACS Biomater Sci Eng*. 2018;4(3):933–941. doi:10.1021/acsbiomaterials.7b00969
39. Reilly GC, Radin S, Chen AT, Ducheyne P. Differential alkaline phosphatase responses of rat and human bone marrow derived mesenchymal stem cells to 45S5 bioactive glass. *Biomaterials*. 2007;28(28):4091–4097. doi:10.1016/j.biomaterials.2007.05.038
40. Uchida M, Oyane A, Kim HM, Kokubo T, Ito A. Biomimetic coating of laminin-apatite composite on titanium metal and its excellent cell-adhesive properties. *Adv Mater*. 2004;16(13):1071. doi:10.1002/adma.200400152
41. Abdallah MN, Badran Z, Ciobanu O, Hamdan N, Tamimi F. Strategies for optimizing the soft tissue seal around osseointegrated implants. *Adv Healthc Mater*. 2017;6(20):1700549. doi:10.1002/adhm.201700549